Regulating π-Conjugation in sp^2-Carbon-Linked Covalent Organic Frameworks for Efficient Metal-Free CO$_2$ Photoreduction with H$_2$O

Lan Yang, Wenkai Yan, Na Yang, Guofeng Wang, Yingpu Bi,* Chengcheng Tian, Honglai Liu,* and Xiang Zhu*

The development of sp^2-carbon-linked covalent organic frameworks (sp^{2}c-COFs) as artificial photocatalysts for solar-driven conversion of CO$_2$ into chemical feedstock has captured growing attention, but catalytic performance has been significantly limited by their intrinsic organic linkages. Here, a simple, yet efficient approach is reported to improve the CO$_2$ photoreduction on metal-free sp^{2}c-COFs by rationally regulating their intrinsic π-conjugation. The incorporation of ethynyl groups into conjugated skeletons affords a significant improvement in π-conjugation and facilitates the photogenerated charge separation and transfer, thereby boosting the CO$_2$ photoreduction in a solid-gas mode with only water vapor and CO$_2$. The resultant CO production rate reaches as high as 382.0 µmol g^{-1} h^{-1}, ranking at the top among all additive-free CO$_2$ photoreduction catalysts. The simple modulation approach not only enables to achieve enhanced CO$_2$ reduction performance but also simultaneously gives a rise to extend the understanding of structure-property relationship and offer new possibilities for the development of new π-conjugated COF-based artificial photocatalysts.

1. Introduction

Photocatalytic conversion of carbon dioxide (CO$_2$) into fuels or value-added chemicals with inexhaustible solar energy is a promising strategy to mitigate climate issues, and simultaneously plays an essential role in solving energy crisis. Toward this end, a wide variety of functional inorganic or organic materials have been developed as artificial photocatalysts for solar-driven reduction of CO$_2$.[1] Among them, synthetic polymers with π-conjugated skeletons have attracted tremendous attention as one of prospective candidates, mainly owing to their strong light-harvesting capacities and tunable organic linkages.[2] Specially, emerged as a new family of crystalline polymers, covalent organic frameworks (COFs) with robust ordered porous architectures and extended π-conjugation come into sight and garner a surge of interests as attractive artificial photocatalysts.[3] A large number of COFs with distinct porosities and functional groups have been built and examined for photocatalytic CO$_2$ reduction, aiming at mimicking natural photosynthesis.[4] Nevertheless, majority of them are constructed following the typical Schiff-base chemistry, where the existence of rich C=N moieties may result in intrinsic low conjugation degree and chemical stability.[5] It has been well documented that π-conjugation plays a key role in modulating the delocalization of π-electrons, improving charge migration efficiency, and achieving enhanced light harvest capacity.[6] In this regard, the search and development of novel crystalline fully-conjugated sp^2-carbon-linked COFs (sp^{2}c-COFs) offers unprecedented opportunities to better convert CO$_2$ into valuable chemicals using solar energy.[7] Recently, Copper's group pioneered the first successful use of a sp^{2}c-COF for the photocatalytic CO$_2$ reduction with an ultra-high CO formation rate of 1040 mmol g^{-1} h^{-1}, where a rhenium complex, [Re(CO)$_5$Cl], was incorporated into the porous matrix to form the desired active sites.[8] Apparently, one key drawback associated with this new type of artificial system lies in the use of a sacrificial agent and preloaded noble-metal cocatalyst, limiting their potential scale-up preparation and application. Thus far, only a few successful attempts of polymeric materials were reported for solar-driven CO$_2$ conversion without sacrificial agents and cocatalysts.[9] The

L. Yang, H. Liu
State Key Laboratory of Chemical Engineering
School of Chemistry and Molecular Engineering
East China University of Science and Technology
Shanghai 200237, P. R. China
E-mail: hlliu@ecust.edu.cn

W. Yan, Y. Bi
State Key Laboratory for Oxo Synthesis and Selective Oxidation
National Engineering Research Center for Fine Petrochemical Intermediates
Lanzhou Institute of Chemical Physics
Chinese Academy of Sciences
Lanzhou 730000, P. R. China
E-mail: yingpubi@licp.cas.cn

N. Yang, G. Wang, X. Zhu
State Key Laboratory for Oxo Synthesis and Selective Oxidation
Suzhou Research Institute of Lanzhou Institute of Chemical Physics
Chinese Academy of Sciences
Suzhou 215000, P. R. China
E-mail: xiang@licp.cas.cn

C. Tian
School of Resources and Environment Engineering
East China University of Science and Technology
Shanghai 200237, P. R. China

development of new metal-free conjugated crystalline polymers for efficient CO_2 photoreduction is of great interest and urgency.

Herein, we report a facile modulation of π-conjugation in metal-free sp^2c-COF-based artificial photocatalysts to achieve enhanced solar-driven CO_2 reduction with H_2O. There is no requirement of the assistance of any extra additives thorough the whole catalytic process. Our key idea is to employ an ethynyl-bridged bond, in conjugation with the triazine ring, to regulate the planarity of a C3-type aldehyde building block, with an aim at the improvement of intrinsic π-conjugation degree of the resulting sp^2c-COF. The presence of these ethynyl units along π-conjugated skeletons can significantly promote the photogenerated charge separation and transfer, thereby affording enhanced CO_2 photoreduction in a solid-gas mode with only water vapor and CO_2. The resultant carbon monoxide (CO) production rate for this metal-free ethynyl-linked sp^2c-COF reaches as high as 382.0 $\mu mol\ g^{-1}\ h^{-1}$, ranking at the top among all additive-free CO_2 photoreduction catalysts.[9e,f,10] This simple modulation approach, leveraging the adjustable synthetic nature of COF linkages, not only enables us to obtain promising CO_2 photoreduction performance but also simultaneously provides a means to extend our understanding of the structure-property relationship of COF-based artificial photocatalysts and applies this understanding to develop highly efficient π-conjugated COFs with potential applications in the solar-driven conversion of CO_2 into chemical feedstock.

2. Results and Discussion

In our attempt at sp^2c-COF photocatalysts, a typical [C3+C3] synthetic approach was adopted, based on a base-promoted aldol condensation reaction between 2,4,6-trimethyl-s-triazine (TMT) and aromatic aldehyde building blocks.[11] A task-specific ethynyl-bridged C3-type monomer, 4,4'',4'''-(benzene-1,3,5-triyltris(ethyne-2,1-diyl))tribenzaldehyde (BTE-TBD) was rationally prepared,[12] on account of its intrinsic planar structural nature, which can be supported by the density functional theory (DFT) calculation (**Scheme 1**). In contrast, the controlled aldehyde monomer, 2,4,6-tris(4-formylphenyl)-1,3,5-benzene (TFPB), exhibits an obvious nonplanar optimized structure with large dihedral angles ranging from 36° to 40°. We speculated that this difference may result in different π-conjugation within the resulting two sp^2c-COF since the coplanarity degree of the polymeric chains significantly affects the delocalization of electrons and the corresponding conjugation degree.[6a,13] Additionally, the frontier molecular orbitals of optimized fragments of these two conjugated sp^2c-COFs (BTE-TBD-COF and TFPB-COF) were also studied (Figure S1, Supporting Information), where HOMOs (the highest occupied molecular orbital) of two structures were mainly distributed above the π-conjugated phenyl-based regions and LUMOs (the lowest unoccupied molecular orbital) were localized surrounding the triazine rings. The theoretical calculated bandgap of BTE-TBD-COF (2.12 eV) is narrower than that of TFPB-COF (2.36 eV), suggesting enhanced π-conjugation within ethynyl-bridged BTE-TBD-COF.

Based on these theoretical results, we then performed detailed COF synthesis. To obtain desired BTE-TBD-COF, BTE-TBD and TMT were added into a Pyrex tube, and a mixed solvent system containing n-butanol and 1,2-dichlorobenzene was employed for the growth of crystalline framework (Scheme 1a). 4 M KOH was required to promote this aldol condensation. The tube was then flash frozen at 77 K and flame sealed under vacuum. The pale-yellow mixture was heated at
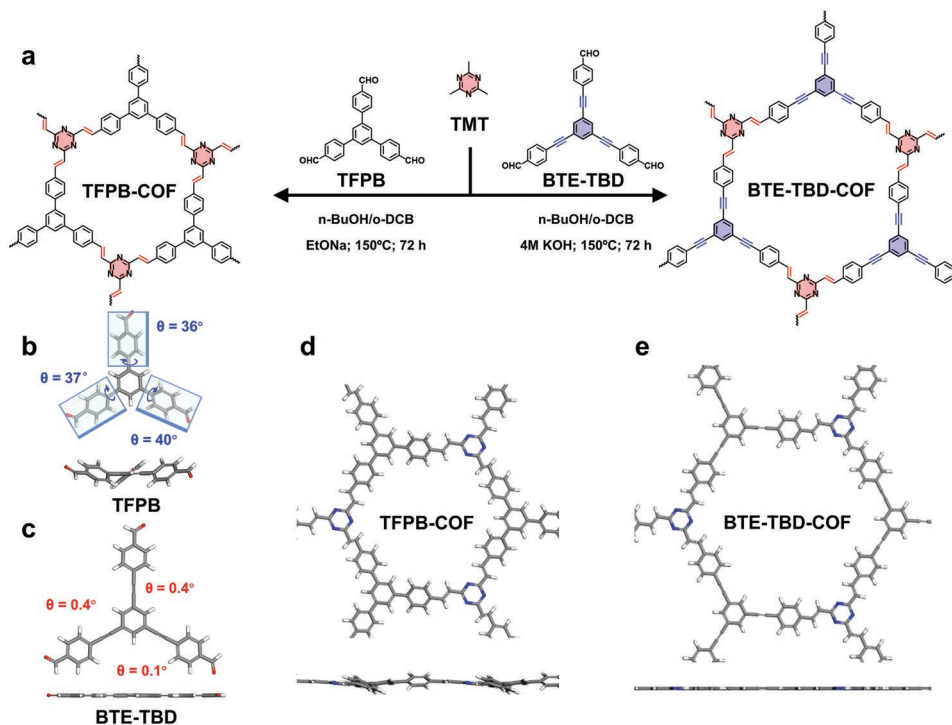
Scheme 1. a) Synthesis routes for sp^2c-COFs (TFPB-COF and BTE-TBD-COF); b–e) theoretical models of aldehyde monomers and COF structures.

150 °C for 72 h. After simple washing and drying processes, the product was achieved with a yield of 81%. A similar procedure was adopted for the generation of controlled TFPB-COF as well,[7c,14] and details can be found in the supporting information.

The chemical structures of the resultant polymers were subsequently studied using Fourier transform infrared spectroscopy (FT-IR) and ^{13}C cross polarization magic angle spinning nuclear magnetic resonance (CP/MAS ^{13}C-NMR) spectroscopy (Figure S2, Supporting Information). Importantly, the appearance of new characteristic stretching vibration peaks of sp^2-carbon linkages (−C=C−) at ca. 1630 and 980 cm^{-1} was be clearly observed for the ethynyl-bridged BTE-TBD-COF, suggesting a successful condensation reaction.[7c,15] This result was further confirmed by the CP/MAS ^{13}C-NMR result, where two distinct peaks, assigned to the phenylene and sp^2-carbon, were founded between 140 and 120 ppm, respectively.[16] The signal ≈170 ppm is typically ascribed to the carbon atoms of the triazine core.[17] The existence of functional ethynyl units can be supported by the signal at ca. 90 ppm.[12c,18] High thermal stability of this ethynyl-linked sp^{2}c-COF can be revealed by the corresponding thermogravimetry analysis (TGA) under the nitrogen atmosphere (Figure S3, Supporting Information).

The powder X-ray diffraction (XRD) patterns of these two COFs were subsequently collected, aiming at their crystalline properties. As expected, a distinguishable peak at 4.8°, corresponding to the reflection from the (100) plane, was obtained for BTE-TBD-COF, where TFPB-COF exhibited an intense peak at 5.9° (**Figure 1**). According to Pawley refinements, the result of BTE-TBD-COF from an eclipsed AA-stacking model

($a = b = 23.28$ Å, $c = 3.49$ Å; $R_p = 3.93\%$, $R_{wp} = 5.74\%$) matched well with the experimental patterns. For TFPB-COF, optimized parameters ($a = b = 18.78$ Å and $c = 3.63$ Å) were obtained and consistent with that of simulated AA-stacking model ($R_p = 3.16\%$; $R_{wp} = 4.93\%$) as well. Different sizes of intrinsic hexagonal structures may account for the as-obtained XRD differences. We then carried out the N$_2$ adsorption–desorption experiments at 77 K to evaluate the porosities of both BTE-TBD-COF and TFPB-COF (Figure S4, Supporting Information). The BET surface area of the former calculated over a relative pressure was 490 m^2 g^{-1} and the pore volume was estimated to be 0.39 cm^3 g^{-1}, where the latter exhibited a similar porous property, with a BET surface area of 544 m^2 g^{-1} and a pore volume of 0.39 cm^3 g^{-1}, respectively. Taken together, all aforementioned results confirmed a successful preparation of porous ethynyl-bridged BTE-TBD-COF and controlled TFPB-COF.

To get a better understanding of the modulation of π-conjugation between these two sp^{2}c-COFs, their optical features were examined by the UV–vis diffuse reflectance spectroscopy (DRS). As shown in **Figure 2**a, broad light absorption was observed for both polymers, where a red-shifted light absorption edge was shown in the spectra of BTE-TBD-COF, as compared to that of TFPB-COF. We reasoned that the resulting different light-harvesting ability could be due to the presence of ethynyl groups within the polymeric architecture, which gave a rise to regulate their inherent conjugation degrees.[19] Based on Tauc plots (Figure 2b), the bandgap (E_g) was determined to be 2.69 eV for BTE-TBD-COF, which was close to its theoretical value and lower than that measured for TFPB-COF (2.77 eV). The band positions were then measured
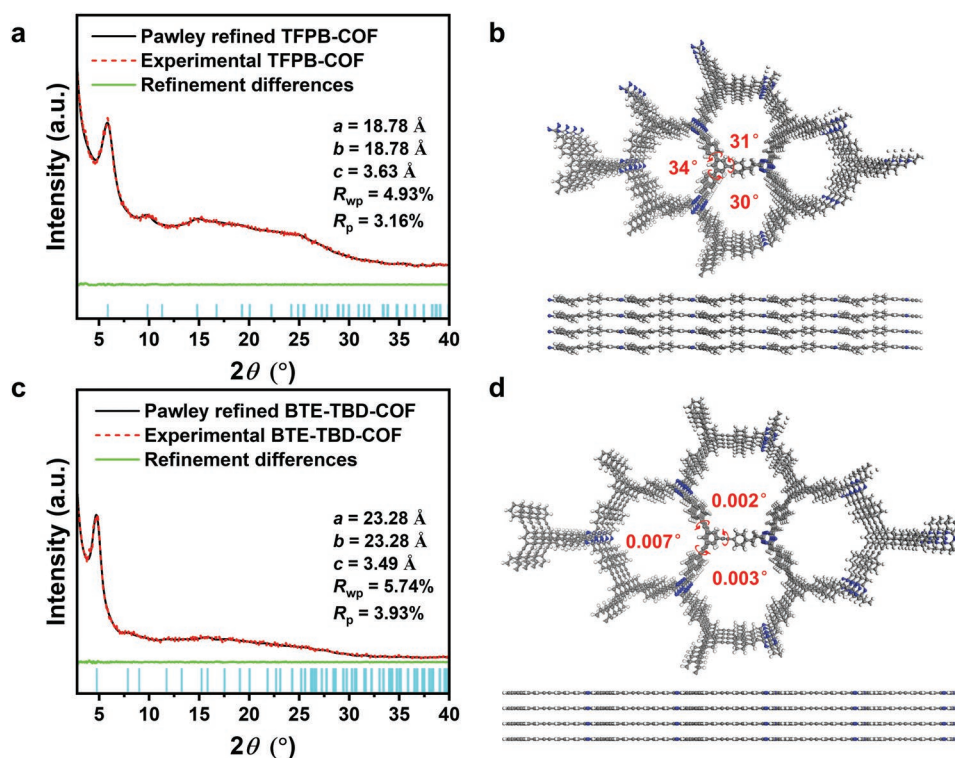

Figure 1. Crystalline structures of TFPB-COF and BTE-TBD-COF. a) XRD patterns of TFPB-COF. b) Simulated space filling AA-stacking model of TFPB-COF. c) XRD patterns of BTE-TBD-COF. d) Simulated space filling AA-stacking model of BTE-TBD-COF.
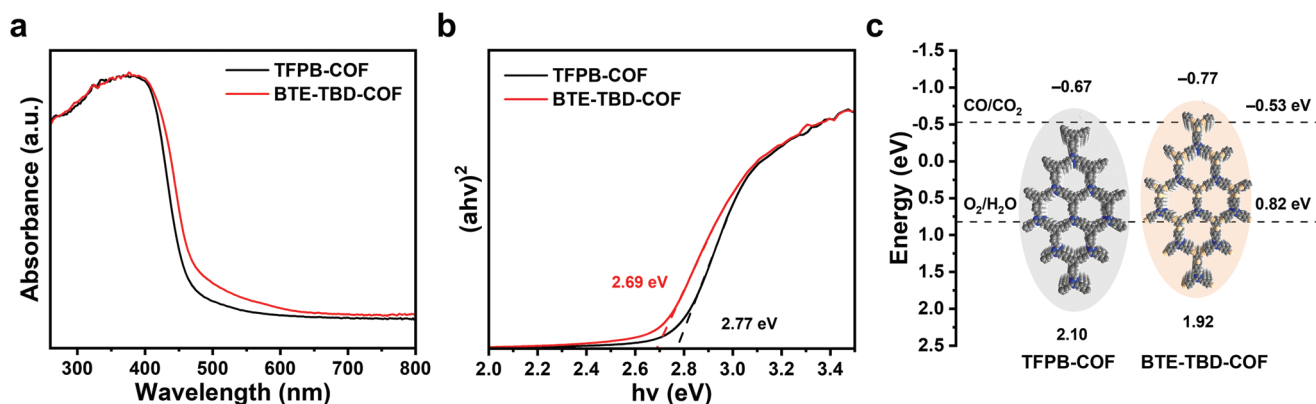
ADVANCED
SCIENCE NEWS
www.advancedsciencenews.com

NANO · MICRO
small
www.small-journal.com

Figure 2. Optical properties of TFPB-COF and BTE-TBD-COF. a) UV–vis DRS spectra. b) Tauc plots. c) Band structures diagram.

and calculated by valence band X-ray photoelectron spectra (VB-XPS, Figure S5, Supporting Information).[20] The valence band position ($E_{VB, XPS}$) of BTE-TBD-COF was determined to be 2.16 eV, and its corresponding VB positions versus the standard hydrogen electrode ($E_{VB, NHE}$) was calculated to be 1.92 eV.[21] Combined with the bandgap result, its conduction band (CB) position ($E_{CB, NHE}$) was estimated to be −0.77 eV,[22] which was larger than that of TFPB-COF ($E_{CB, NHE}$ = −0.67 eV). Moreover, this value was more negative than the redox position of CO_2 to CO (CO_2/CO, −0.53 eV vs NHE, pH = 7), where its VB position was positive enough to oxidize water (O_2/H_2O, 0.82 eV vs NHE,

pH = 7), implying the sufficient redox ability of ethynyl-bridged BTE-TBD-COF to trigger the photocatalytic reduction of CO_2 (Figure 2c). As a result, the successful incorporation of ethynyl moieties into π-conjugated skeletons provided a facile means to regulating the conjugation degree thorough the aromatic framework, which may offer new opportunities for developing π-conjugated COFs.

Inspired by the above results, the photocatalytic reduction of CO_2 with gaseous H_2O under simulated sunlight irradiation (λ = 320 − 780 nm) using BTE-TBD-COF as a metal-free catalyst was initiated. No photosensitizers, sacrificial agents,
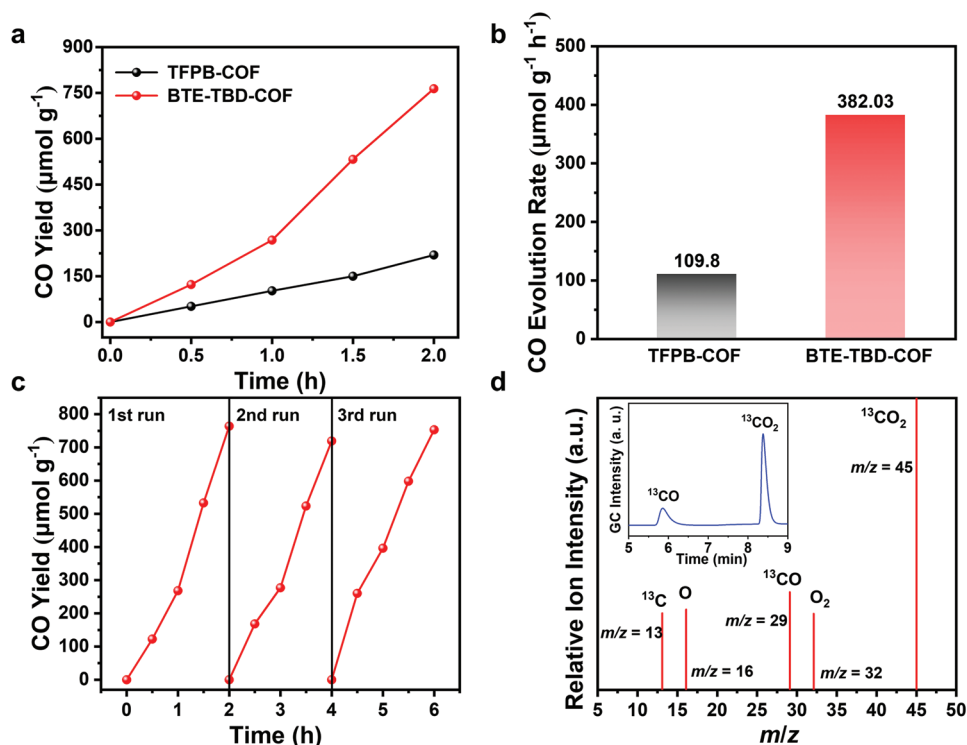

Figure 3. Photocatalytic carbon dioxide reduction performance of TFPB-COF and BTE-TBD-COF. a) Time courses of CO production during 2 h experiment. b) CO evolution rate. c) Cycling production of CO using BTE-TBD-COF as the photocatalyst. d) Mass spectrum of [13]CO obtained from the photocatalytic CO_2 reduction under [13]CO_2 atmosphere using BTE-TBD-COF as the artificial photocatalyst (inset: the corresponding gas chromatography (GC) spectrum).

and cocatalysts were utilized during the whole measurement. Interestingly, gaseous CO was detected as the only reductive product, where a remarkable CO evolution rate of 382.03 $\mu mol\ g^{-1}\ h^{-1}$ was achieved after the two-hour irradiation of simulated sunlight for ethynyl-bridged BTE-TBD-COF (**Figure 3**a,b). This activity was significantly better than that of TFPB-COF (109.8 $\mu mol\ g^{-1}\ h^{-1}$), and ranked at the top among all additive-free polymeric catalysts (Table S1, Supporting Information).[9,10] The apparent quantum yield (AQY) for CO evolution of BTE-TBD-COF was measured to be 0.11% at 405 nm (Figure S6, Supporting Information).[9b,23] Moreover, the catalytic performance can maintain as high as 96% after three cycles (Figure 3c), where the chemical stability of BTE-TBD-COF was well-preserved, as evidenced by its XRD patterns, FT-IR spectra, and UV–vis DRS results before and after the catalysis process (Figure S7, Supporting Information). To further confirm the as-obtained photocatalytic activity, a series of control experiments were carried out, where no CO can be formed in the absence of CO_2, light source, or the COF catalyst. In addition, the isotope labeling experiments successfully proved that the carbon source of the CO product merely originated from the CO_2 reactant and revealed the presence of $^{18}O_2$ ($m/z = 36$) (Figure 3d; Figure S8, Supporting Information), confirming that CO and O_2 were generated from the photocatalytic CO_2 reduction reaction.

In situ diffuse reflectance infrared Fourier transform spectroscopy (DRIFTS) was then attempted to reveal the catalytic mechanism. As shown in **Figure 4**b, CO_2 molecules adsorbed on the surface of BTE-TBD-COF can capture an electron to form the CO_2^- (at 1655 and 1613 cm^{-1}) species. Typical carbon species, such as b-CO_3^{2-} (1561, 1228 cm^{-1}), m-CO_3^{2-} (1306 cm^{-1}), and HCO_3^- (1440 cm^{-1}), were also formed due to the chemical adsorption of CO_2 and physical adsorption of H_2O or hydrogen bonding interaction.[10h] In addition, the peak of COOH* species (1724 cm^{-1}), the key intermediate for a successful reduction of CO_2 to CO,[10e,h] was observed and gradually strengthened along with light irradiation. As a result, gaseous CO product can be formed through further conversion of COOH* under the irradiation of simulated sunlight.[10]

Given the high catalytic activity of BTE-TBD-COF, which was about three times larger than that of TFPB-COF, we subsequently initiated a series of physiochemical characterizations to get deeper insights of this enhancement. First, the CO_2 uptake of both sp^2c-COFs was assessed at 273 K (Figure S9, Supporting Information), where TFPB-COF exhibited a higher CO_2 adsorption (41 $cm^3\ g^{-1}$) in comparison with that of BTE-TBD-COF (28 $cm^3\ g^{-1}$), which could be due to its larger BET surface area. In this regard, we speculated that the difference in their π-conjugation could play a crucial role in achieving the resulting enhanced CO_2 photoreduction performance on the ethynyl-bridged BTE-TBD-COF. To confirm this, their photoelectrochemical responses were measured, and the photocurrent density of BTE-TBD-COF was determined to be evidently larger than that obtained for TFPB-COF (Figure 4c), suggesting enhanced photoinduced charge separation and transport.[7b,24] Additionally, the electrochemical impendence spectrum (EIS) of BTE-TBD-COF showed a smaller semicircle
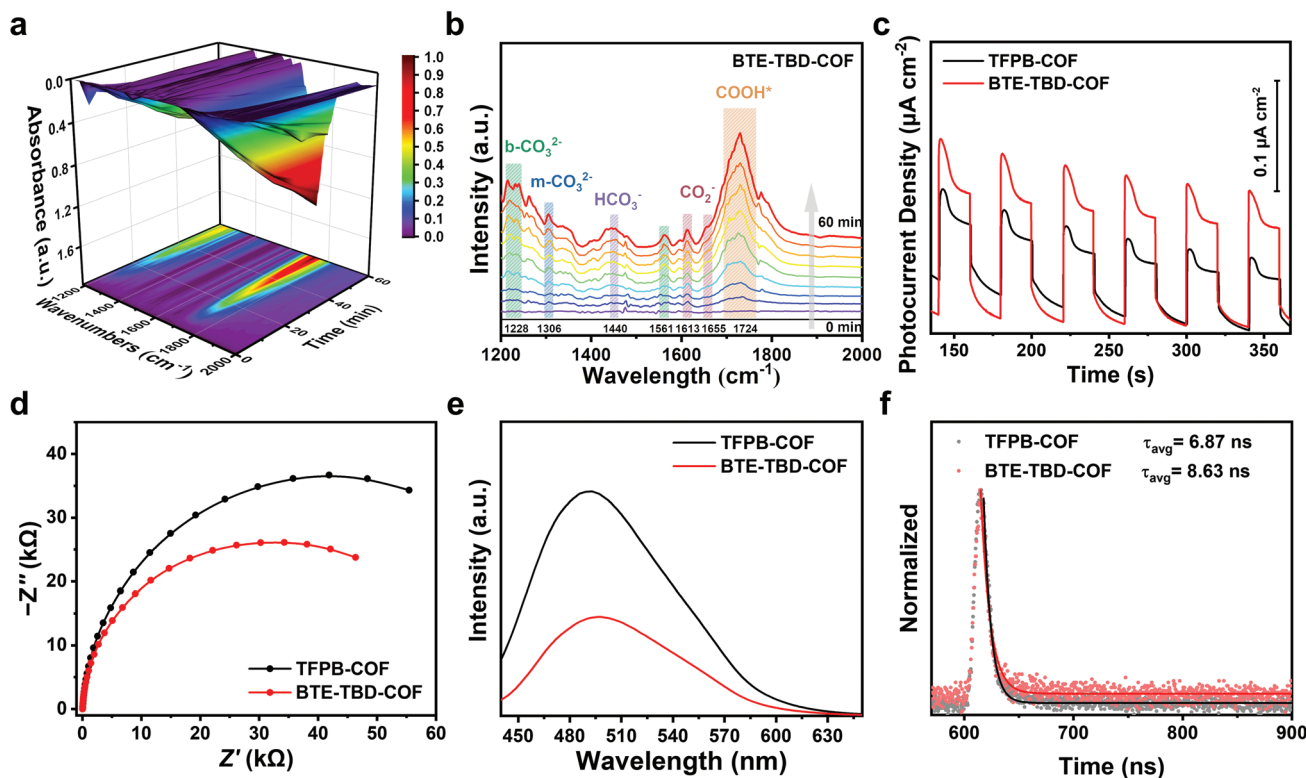

Figure 4. In situ DRIFTS spectra of BTE-TBD-COF and charge separation behaviors of TFPB-COF and BTE-TBD-COF. a,b) In situ DRIFTS spectra of BTE-TBD-COF. c) Transient photocurrent measurements. d) EIS Nyquist plots . e) PL spectra with the excitation wavelength of 564 nm. f) Time-resolved fluorescence decay spectra.

radius than that of TFPB-COF (Figure 4d), indicating that BTE-TBD-COF bore a lower electric charge transfer resistance.[25] Apparently, it could help to promote the migration of photogenerated charge carries, affording an enhanced catalytic activity. Furthermore, the stable-state photoluminescence (PL) spectrum was also recorded (Figure 4e), and a weaker peak was observed for BTE-TBD-COF, as compared to that of TFPB-COF, verifying a more effective suppression of photogenerated carriers recombination.[4b,26] This result was consistent with that obtained from time-resolved fluorescence decay spectroscopy (Figure 4f; and Table S4, Supporting Information), where the average fluorescence lifetime of BTE-TBD-COF (8.63 ns) was much longer than TFPB-COF (6.87 ns), further confirming its higher separation efficiency of photoinduced charge carries. Taken together, regulating intrinsic π-conjugation in 2D sp^2c-COFs gave a facile rise to modulating their photoelectrochemical properties, so as to turn their CO_2 photoreduction performance.

According to the above-mentioned experimental and theoretical results, the possible CO_2 photoreduction process for BTE-TBD-COF can be described as follows: The CO_2 gas was first adsorbed by porous ethynyl-bridged BTE-TBD-COF. Upon the illumination of simulated sunlight, the photogenerated electrons (e^-) could migrate from the HOMO level to the LUMO level of the COF. Subsequently, the adsorbed CO_2 molecules could capture electrons on the COF surface to generate CO and H_2O ($CO_2 + 2H^+ + 2e^- \rightarrow CO + H_2O$), where the photoinduced holes were utilized for oxidizing water to form oxygen and hydrogen ions through the half-reaction ($2H_2O + 4h^+ \rightarrow O_2 + 4H^+$). The low water concentration could efficiently inhibit the competitive reaction, thereby leading to a high selectivity for our BTE-TBD-COF.

3. Conclusion

In conclusion, a simple, yet efficient approach was developed to improve solar-driven CO_2 reduction performance on metal-free sp^2c-COF-based artificial photocatalysts by regulating their intrinsic π-conjugation. Rational incorporation of ethynyl groups into conjugated skeletons within the architectures of COFs affords a significant improvement in π-conjugation and facilitates the photogenerated charge separation and transfer, thereby boosting the CO_2 photoreduction in a solid-gas mode with only water vapor and CO_2. The resultant CO production rate on the ethynyl-bridged sp^2c-COF (BTE-TBD-COF) reaches as high as 382.0 µmol g^{-1} h^{-1}, ranking at the top among all additive-free CO_2 photoreduction catalysts. In addition to the obtained high activity, this approach also provides a means to extend our understanding of structure-property relationship. We anticipate this study may offer new possibilities for the rational design and synthesis of new π-conjugated COFs for photocatalytic applications.

Supporting Information

Supporting Information is available from the Wiley Online Library or from the author.

Conflict of Interest

The authors declare no conflict of interest.

Data Availability Statement

The data that support the findings of this study are available in the supplementary material of this article.

[1] a) C. Wang, Z. Sun, Y. Zheng, Y. H. Hu, *J. Mater. Chem. A* **2019**, *7*, 865; b) A. Behera, A. K. Kar, R. Srivastava, *Mater. Horiz.* **2022**, *9*, 607.

[2] a) G. Singh, J. Lee, A. Karakoti, R. Bahadur, J. Yi, D. Zhao, K. AlBahily, A. Vinu, *Chem. Soc. Rev.* **2020**, *49*, 4360; b) M. G. Mohamed, A. F. M. El-Mahdy, M. G. Kotp, S.-W. Kuo, *Mater. Adv.* **2022**, *3*, 707.

[3] a) H. Wang, H. Wang, Z. Wang, L. Tang, G. Zeng, P. Xu, M. Chen, T. Xiong, C. Zhou, X. Li, D. Huang, Y. Zhu, Z. Wang, J. Tang, *Chem. Soc. Rev.* **2020**, *49*, 4135; b) C. Xia, K. O. Kirlikovali, T. H. C. Nguyen, X. C. Nguyen, Q. B. Tran, M. K. Duong, M. T. Nguyen Dinh, D. L. T. Nguyen, P. Singh, P. Raizada, V.-H. Nguyen, S. Y. Kim, L. Singh, C. C. Nguyen, M. Shokouhimehr, Q. V. Le, *Coord. Chem. Rev.* **2021**, *446*, 214117; c) R. Sani, T. K. Dey, M. Sarkar, P. Basu, S. M. Islam, *Mater. Adv.* **2022**, *3*, 5575; d) C.-X. Chen, Y.-Y. Xiong, X. Zhong, P. C. Lan, Z.-W. Wei, H. Pan, P.-Y. Su, Y. Song, Y.-F. Chen, A. Nafady, Sirajuddin, S. Ma, *Angew. Chem., Int. Ed.* **2022**, *61*, 202114071; e) Z. Zhao, Y. Zheng, C. Wang, S. Zhang, J. Song, Y. Li, S. Ma, P. Cheng, Z. Zhang, Y. Chen, *ACS Catal.* **2021**, *11*, 2098; f) J. Yang, S. Ghosh, J. Roeser, A. Acharjya, C. Penschke, Y. Tsutsui, J. Rabeah, T. Wang, S. Y. Djoko Tameu, M.-Y. Ye, J. Grüneberg, S. Li, C. Li, R. Schomäcker, R. Van De Krol, S. Seki, P. Saalfrank, A. Thomas, *Nat. Commun.* **2022**, *13*, 6317.

[4] a) M. Lu, M. Zhang, J. Liu, Y. Chen, J.-P. Liao, M.-Y. Yang, Y.-P. Cai, S.-L. Li, Y.-Q. Lan, *Angew. Chem., Int. Ed.* **2022**, *61*, 202200003; b) L. Zou, R. Sa, H. Zhong, H. Lv, X. Wang, R. Wang, *ACS Catal.* **2022**, *12*, 3550.

[5] a) S. Yang, W. Hu, X. Zhang, P. He, B. Pattengale, C. Liu, M. Cendejas, I. Hermans, X. Zhang, J. Zhang, J. Huang, *J. Am. Chem. Soc.* **2018**, *140*, 14614; b) W. Zhong, R. Sa, L. Li, Y. He, L. Li, J. Bi, Z. Zhuang, Y. Yu, Z. Zou, *J. Am. Chem. Soc.* **2019**, *141*, 7615;

c) W. Liu, X. Li, C. Wang, H. Pan, W. Liu, K. Wang, Q. Zeng, R. Wang, J. Jiang, *J. Am. Chem. Soc.* **2019**, *141*, 17431.

[6] a) H. J. Son, F. He, B. Carsten, L. Yu, *J. Mater. Chem.* **2011**, *21*, 18934; b) P. Deng, Z. Wu, K. Cao, Q. Zhang, B. Sun, S. R. Marder, *Polym. Chem.* **2013**, *4*, 5275; c) L. Bucher, N. Desbois, P. D. Harvey, C. P. Gros, G. D. Sharma, *ACS Appl. Mater. Interfaces* **2018**, *10*, 992; d) C. Ru, T. Zhou, J. Zhang, X. Wu, P. Sun, P. Chen, L. Zhou, H. Zhao, J. Wu, X. Pan, *Macromolecules* **2021**, *54*, 8839.

[7] a) S. Bi, Z.-A. Lan, S. Paasch, W. Zhang, Y. He, C. Zhang, F. Liu, D. Wu, X. Zhuang, E. Brunner, X. Wang, F. Zhang, *Adv. Funct. Mater.* **2017**, *27*, 1703146; b) E. Jin, Z. Lan, Q. Jiang, K. Geng, G. Li, X. Wang, D. Jiang, *Chem* **2019**, *5*, 1632; c) S. Wei, F. Zhang, W. Zhang, P. Qiang, K. Yu, X. Fu, D. Wu, S. Bi, F. Zhang, *J. Am. Chem. Soc.* **2019**, *141*, 14272; d) J. Xu, C. Yang, S. Bi, W. Wang, Y. He, D. Wu, Q. Liang, X. Wang, F. Zhang, *Angew. Chem., Int. Ed.* **2020**, *59*, 23845; e) Z. Zhao, D. Zheng, M. Guo, J. Yu, S. Zhang, Z. Zhang, Y. Chen, *Angew. Chem., Int. Ed.* **2022**, *61*, 202200261; f) Z. Zhao, X. Chen, B. Li, S. Zhao, L. Niu, Z. Zhang, Y. Chen, *Adv. Sci.* **2022**, *9*, 2203832.

[8] Z. Fu, X. Wang, A. M. Gardner, X. Wang, S. Y. Chong, G. Neri, A. J. Cowan, L. Liu, X. Li, A. Vogel, R. Clowes, M. Bilton, L. Chen, R. S. Sprick, A. I. Cooper, *Chem. Sci.* **2020**, *11*, 543.

[9] a) X. Yu, Z. Yang, B. Qiu, S. Guo, P. Yang, B. Yu, H. Zhang, Y. Zhao, X. Yang, B. Han, Z. Liu, *Angew. Chem., Int. Ed.* **2019**, *58*, 632; b) C. Dai, L. Zhong, X. Gong, L. Zeng, C. Xue, S. Li, B. Liu, *Green Chem.* **2019**, *21*, 6606; c) J. You, Y. Zhao, L. Wang, W. Bao, *J. Cleaner Prod.* **2021**, *291*, 125822; d) Y. Wang, G. Ji, W. Ye, F. Zhang, Y. Wang, Y. Zhao, Z. Liu, *ACS Sustainable Chem. Eng.* **2022**, *10*, 9460; e) W. Ye, Y. Wang, G. Ji, F. Zhang, Y. Zhao, Z. Liu, *ChemSusChem* **2022**, *15*, 202200759; f) M. Lu, M. Zhang, J. Liu, T.-Y. Yu, J.-N. Chang, L.-J. Shang, S.-L. Li, Y.-Q. Lan, *J. Am. Chem. Soc.* **2022**, *144*, 1861.

[10] a) H. Yaghoubi, Z. Li, Y. Chen, H. T. Ngo, V. R. Bhethanabotla, B. Joseph, S. Ma, R. Schlaf, A. Takshi, *ACS Catal.* **2015**, *5*, 327; b) J. Wu, X. Li, W. Shi, P. Ling, Y. Sun, X. Jiao, S. Gao, L. Liang, J. Xu, W. Yan, C. Wang, Y. Xie, *Angew. Chem., Int. Ed.* **2018**, *57*, 8719; c) J. Zhou, H. Wu, C.-Y. Sun, C.-Y. Hu, X.-L. Wang, Z.-H. Kang, Z.-M. Su, *J. Mater. Chem. A* **2018**, *6*, 21596; d) M. Lu, J. Liu, Q. Li, M. Zhang, M. Liu, J.-L. Wang, D.-Q. Yuan, Y.-Q. Lan, *Angew. Chem., Int. Ed.* **2019**, *58*, 12392; e) K. Lei, D. Wang, L. Ye, M. Kou, Y. Deng, Z. Ma, L. Wang, Y. Kong, *ChemSusChem* **2020**, *13*, 1725; f) L.-J. Wang, R.-l. Wang, X. Zhang, J.-l. Mu, Z.-Y. Zhou, Z.-M. Su, *ChemSusChem* **2020**, *13*, 2973; g) M. Zhang, M. Lu, Z.-L. Lang, J. Liu, M. Liu, J.-N. Chang, L.-Y. Li, L.-J. Shang, M. Wang, S.-L. Li, Y.-Q. Lan, *Angew. Chem., Int. Ed.* **2020**, *59*, 6500; h) M. Kou, W. Liu, Y. Wang, J. Huang, Y. Chen, Y. Zhou, Y. Chen, M. Ma, K. Lei, H. Xie, P. K. Wong, L. Ye, *Appl. Catal. B* **2021**, *291*, 120146; i) L. Wang, G. Huang, L. Zhang, R. Lian, J. Huang, H. She, C. Liu, Q. Wang, *J. Energy Chem.* **2022**, *64*, 85.

[11] a) H. Lyu, C. S. Diercks, C. Zhu, O. M. Yaghi, *J. Am. Chem. Soc.* **2019**, *141*, 6848; b) A. Acharjya, P. Pachfule, J. Roeser, F.-J. Schmitt, A. Thomas, *Angew. Chem., Int. Ed.* **2019**, *58*, 14865; c) T. Jadhav, Y. Fang, W. Patterson, C.-H. Liu, E. Hamzehpoor, D. F. Perepichka, *Angew. Chem., Int. Ed.* **2019**, *58*, 13753; d) A. Acharjya, L. Longworth-Dunbar, J. Roeser, P. Pachfule, A. Thomas, *J. Am. Chem. Soc.* **2020**, *142*, 14033.

[12] a) R. L. Greenaway, V. Santolini, M. J. Bennison, B. M. Alston, C. J. Pugh, M. A. Little, M. Miklitz, E. G. B. Eden-Rump, R. Clowes, A. Shakil, H. J. Cuthbertson, H. Armstrong, M. E. Briggs, K. E. Jelfs, A. I. Cooper, *Nat. Commun.* **2018**, *9*, 2849; b) K. Cai, W. Wang, J. Zhang, L. Chen, L. Wang, X. Zhu, Z. Yu, Z. Wu, H. Zhou, *J. Mater. Chem. A* **2022**, *10*, 7165; c) L. Zhai, Z. Xie, C.-X. Cui, X. Yang, Q. Xu, X. Ke, M. Liu, L.-B. Qu, X. Chen, L. Mi, *Chem. Mater.* **2022**, *34*, 5232.

[13] a) H. Zhan, S. Lamare, A. Ng, T. Kenny, H. Guernon, W.-K. Chan, A. B. Djurišić, P. D. Harvey, W.-Y. Wong, *Macromolecules* **2011**, *44*, 5155; b) X. Song, W. Zhang, X. Li, H. Jiang, C. Shen, W.-H. Zhu, *J. Mater. Chem. C* **2016**, *4*, 9203.

[14] Q. Guo, H. Ji, L. Yang, D. Ji, Z. Ai, S. Luo, J. Sun, Y. Liu, D. Wei, *Chin. Chem. Lett.* **2022**, *33*, 2621.

[15] a) S. Yang, D. Streater, C. Fiankor, J. Zhang, J. Huang, *J. Am. Chem. Soc.* **2021**, *143*, 1061; b) C. Xu, Q. Xie, W. Zhang, S. Xiong, C. Pan, J. Tang, G. Yu, *Macromol. Rapid Commun.* **2020**, *41*, 2000006.

[16] F. Zhang, S. Wei, W. Wei, J. Zou, G. Gu, D. Wu, S. Bi, F. Zhang, *Sci. Bull.* **2020**, *65*, 1659.

[17] a) A. Acharjya, P. Pachfule, J. Roeser, F. J. Schmitt, A. Thomas, *Angew. Chem., Int. Ed.* **2019**, *58*, 14865; b) X. Zhu, C. Tian, S. M. Mahurin, S.-H. Chai, C. Wang, S. Brown, G. M. Veith, H. Luo, H. Liu, S. Dai, *J. Am. Chem. Soc.* **2012**, *134*, 10478; c) X. Zhu, S. An, Y. Liu, J. Hu, H. Liu, C. Tian, S. Dai, X. Yang, H. Wang, C. W. Abney, S. Dai, *AIChE J.* **2017**, *63*, 3470; d) S. An, X. Zhu, Y. He, L. Yang, H. Wang, S. Jin, J. Hu, H. Liu, *Ind. Eng. Chem. Res.* **2019**, *58*, 10495; e) N. Yang, L. Yang, X. Zhu, P. Zhao, H. Liu, C. Xia, S. Dai, C. Tian, *ACS Mater. Lett.* **2022**, *4*, 2143.

[18] P. Pachfule, A. Acharjya, J. Roeser, T. Langenhahn, M. Schwarze, R. Schomäcker, A. Thomas, J. Schmidt, *J. Am. Chem. Soc.* **2018**, *140*, 1423.

[19] a) P. N. Taylor, A. P. Wylie, J. Huuskonen, H. L. Anderson, *Angew. Chem., Int. Ed.* **1998**, *37*, 986; b) H. L. Anderson, *Chem. Commun.* **1999**, 2323; c) F. Silvestri, A. Marrocchi, M. Seri, C. Kim, T. J. Marks, A. Facchetti, A. Taticchi, *J. Am. Chem. Soc.* **2010**, *132*, 6108; d) K. Gao, L. Li, T. Lai, L. Xiao, Y. Huang, F. Huang, J. Peng, Y. Cao, F. Liu, T. P. Russell, R. A. J. Janssen, X. Peng, *J. Am. Chem. Soc.* **2015**, *137*, 7282.

[20] H. Wang, C. Qian, J. Liu, Y. Zeng, D. Wang, W. Zhou, L. Gu, H. Wu, G. Liu, Y. Zhao, *J. Am. Chem. Soc.* **2020**, *142*, 4862.

[21] X. Li, B. Kang, F. Dong, Z. Zhang, X. Luo, L. Han, J. Huang, Z. Feng, Z. Chen, J. Xu, B. Peng, Z. L. Wang, *Nano Energy* **2021**, *81*, 105671.

[22] J. Liu, Y. Liu, N. Liu, Y. Han, X. Zhang, H. Huang, Y. Lifshitz, S.-T. Lee, J. Zhong, Z. Kang, *Science* **2015**, *347*, 970.

[23] a) Q. Han, X. Bai, Z. Man, H. He, L. Li, J. Hu, A. Alsaedi, T. Hayat, Z. Yu, W. Zhang, J. Wang, Y. Zhou, Z. Zou, *J. Am. Chem. Soc.* **2019**, *141*, 4209; b) Q. Niu, S. Dong, J. Tian, G. Huang, J. Bi, L. Wu, *ACS Appl. Mater. Interfaces* **2022**, *14*, 24299; c) M. Lu, M. Zhang, J. Liu, T.-Y. Yu, J.-N. Chang, L.-J. Shang, S.-L. Li, Y.-Q. Lan, *J. Am. Chem. Soc.* **2022**, *144*, 1861; d) Z. Tang, S. Xu, N. Yin, Y. Yang, Q. Deng, J. Shen, X. Zhang, T. Wang, H. He, X. Lin, Y. Zhou, Z. Zou, *Adv. Mater.* **2023**, 2210693.

[24] a) C.-C. Li, M.-Y. Gao, X.-J. Sun, H.-L. Tang, H. Dong, F.-M. Zhang, *Appl. Catal. B* **2020**, *266*, 118586; b) Y. Zhang, Z. Xu, Q. Wang, W. Hao, X. Zhai, X. Fei, X. Huang, Y. Bi, *Appl. Catal. B* **2021**, *299*, 120679.

[25] a) K. Chen, M. Cao, Y. Lin, J. Fu, H. Liao, Y. Zhou, H. Li, X. Qiu, J. Hu, X. Zheng, M. Shakouri, Q. Xiao, Y. Hu, J. Li, J. Liu, E. Cortés, M. Liu, *Adv. Funct. Mater.* **2022**, *32*, 2111322; b) Q. Wang, K. Liu, K. Hu, C. Cai, H. Li, H. Li, M. Herran, Y.-R. Lu, T.-S. Chan, C. Ma, J. Fu, S. Zhang, Y. Liang, E. Cortés, M. Liu, *Nat. Commun.* **2022**, *13*, 6082; c) Q. Chen, K. Liu, Y. Zhou, X. Wang, K. Wu, H. Li, E. Pensa, J. Fu, M. Miyauchi, E. Cortés, M. Liu, *Nano Lett.* **2022**, *22*, 6276; d) S. Chen, X. Li, C.-W. Kao, T. Luo, K. Chen, J. Fu, C. Ma, H. Li, M. Li, T.-S. Chan, M. Liu, *Angew. Chem., Int. Ed.* **2022**, *61*, 202206233.

[26] a) L. Chen, L. Wang, Y. Wan, Y. Zhang, Z. Qi, X. Wu, H. Xu, *Adv. Mater.* **2020**, *32*, 1904433; b) C.-R. Zhang, W.-R. Cui, R.-H. Xu, X.-R. Chen, W. Jiang, Y.-D. Wu, R.-H. Yan, R.-P. Liang, J.-D. Qiu, *CCS Chem.* **2021**, *3*, 168.